

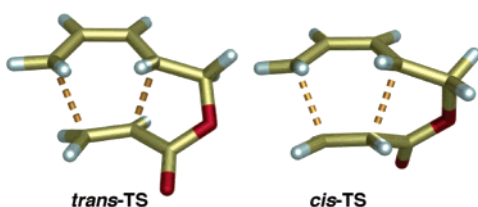
Intramolecular Diels–Alder Reactions of Ester-Linked 1,3,8-Nonatrienes

Tory N. Cayzer,[†] Michael N. Paddon-Row,^{*,‡} Damian Moran,[‡] Alan D. Payne,[†]
Michael S. Sherburn,^{*,†} and Peter Turner^{§,||}

Research School of Chemistry, Australian National University, Canberra, ACT 0200, Australia, School of Chemistry, The University of New South Wales, Sydney, NSW 2052, Australia, and School of Chemistry, University of Sydney, Sydney, NSW 2006, Australia

sherburn@rsc.anu.edu.au; m.paddonrow@unsw.edu.au

Received March 22, 2005



Penta-1,3-dienyl acrylates undergo kinetically controlled intramolecular Diels–Alder (IMDA) reactions and DFT calculations (B3LYP/6-31+G(d)) predict stereoselectivities that are in very good agreement with the experimental values. The nature of the diene C1 substituent has virtually no influence upon reactivity or trans/cis-stereoselectivity whereas terminal C9 dienophile substituents have a substantial effect on both the reactivity and stereoselectivity of these IMDA reactions. The TSs highlight contributions from strain in the developing tether-containing ring, and steric and electronic effects between tether and dienophile substituents, thus providing insight into the origins of IMDA reactivity and stereoselectivity.

Introduction

The continuing popularity of the intramolecular Diels–Alder reaction (IMDA) in synthesis stems from its uncommon power: two rings, two covalent bonds and up to four stereocenters are generated in a single bond-forming event (e.g., **1–19**; Scheme 1).¹ Despite notable contributions,^{2–6} the endo/exo-⁷ and π -facial stereocon-

trolling features of many IMDAs remain either unknown or unproven. Our continuing studies^{8–13} involve a combined computational/synthetic approach¹⁴ to the development of a deeper understanding of the intramolecular Diels–Alder reaction. We recently demonstrated that, contrary to many literature reports, pentadienyl acrylates readily undergo IMDAs between 132 and 180 °C.¹¹ For example, while the parent system **1** undergoes a mildly cis-selective cycloaddition, the presence of C3–Br and C5–CH₃ groups (Figure 1) led to more facile and more

* Corresponding author.

[†] Australian National University.

[‡] The University of New South Wales.

[§] University of Sydney.

^{||} Author to whom correspondence should be addressed regarding crystal structures: p.turner@chem.usyd.edu.au.

(1) Reviews on the IMDA: (a) Taber, D. F. *Intramolecular Diels–Alder and Alder Ene Reactions*; Springer-Verlag: Berlin, 1984. (b) Fallis, A. G. *Can. J. Chem.* **1984**, *62*, 183–234. (c) Ciganek, E. *Org. React.* **1984**, *32*, 1–374. (d) Craig, D. *Chem. Soc. Rev.* **1987**, *16*, 187–238. (e) Roush, W. R. In *Advances in Cycloaddition*; Curran, D. P., Ed.; JAI: Greenwich, CT, 1990; Vol. 2, pp 91–146. (f) Roush, W. R. In *Comprehensive Organic Synthesis*; Trost, B. M., Fleming, I., Paquette, L. A., Eds.; Pergamon: Oxford, 1991; Vol. 5, pp 513–550. (g) Craig, D. In *Stereoselective Synthesis*, 4th ed.; Helmchen, G., Hoffmann, R. W., Mulzer, J., Schumann, E., Eds.; Methods of Organic Chemistry (Houben-Weyl) No. E21c; Thieme: Stuttgart, 1995; pp 2872–2904.

(2) Tantillo, D. J.; Houk, K. N.; Jung, M. E. *J. Org. Chem.* **2001**, *66*, 1938–1940.

(3) Diedrich, M. K.; Klaerner, F.-G.; Beno, B. R.; Houk, K. N.; Senderowitz, H.; Still, W. C. *J. Am. Chem. Soc.* **1997**, *119*, 10255–10259.

(4) Brown, F. K.; Singh, U. C.; Kollman, P. A.; Raimondi, L.; Houk, K. N.; Bock, C. W. *J. Org. Chem.* **1992**, *57*, 4862–4869.

(5) Raimondi, L.; Brown, F. K.; Gonzalez, J.; Houk, K. N. *J. Am. Chem. Soc.* **1992**, *114*, 4796–4804.

(6) Brown, F. K.; Houk, K. N. *Tetrahedron Lett.* **1985**, *26*, 2297–2300.

(7) We use the terms cis and trans in place of endo and exo to identify TSs and products. Endo and exo are ambiguous terms when describing TSs and products of *E*-1,2-disubstituted dienophiles.

(8) Lilly, M. J.; Paddon-Row, M. N.; Sherburn, M. S.; Turner, C. I. *Chem. Commun.* **2000**, 2213–2214.

(9) Paddon-Row, M. N.; Sherburn, M. S. *Chem. Commun.* **2000**, 2215–2216.

(10) Turner, C. I.; Williamson, R. M.; Paddon-Row, M. N.; Sherburn, M. S. *J. Org. Chem.* **2001**, *66*, 3963–3969.

(11) Cayzer, T. N.; Wong, L. S.-M.; Turner, P.; Paddon-Row, M. N.; Sherburn, M. S. *Chem. Eur. J.* **2002**, *8*, 739–750.

(12) Jones, G. A.; Paddon-Row, M. N.; Sherburn, M. S.; Turner, C. I. *Org. Lett.* **2002**, *4*, 3789–3792.

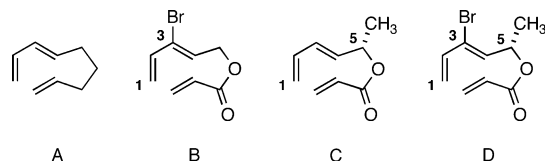
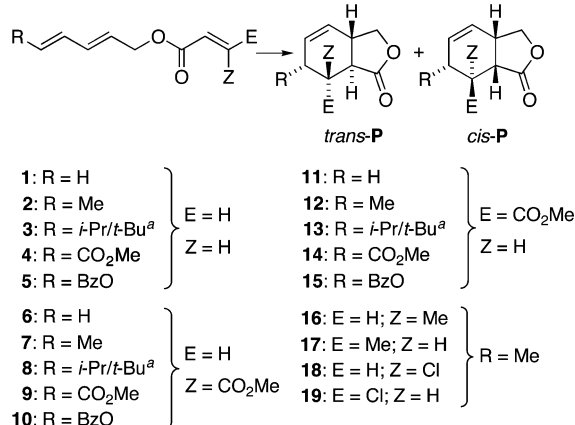


FIGURE 1. 1,3,8-Nonatriene (A) and ester-tethered C3 and C4-substituted cognates (B–D).

SCHEME 1. Intramolecular Diels–Alder Reaction *trans*- and *cis*-Bicyclic Products



^aThe *i*-Pr and *t*-Bu groups were employed during experiments and DFT studies, respectively.

trans-selective IMDAs.¹⁶ Pentadienyl maleates (**6**, **7**) and fumarates (**11**, **12**) (Scheme 1) also undergo IMDAs at 80–110 °C.^{8,17,18} The thermodynamically less stable

trans-fused cycloadducts are formed predominantly, irrespective of the dienophile geometry. The maleate *Z*-dienophiles furnish more *trans*-selective IMDAs because of destabilizing overlap repulsion in the TSs leading to the *E*-dienophile series *trans*-adducts.⁸

Herein, ester-tethered 1,3,8-nonatrienes^{19–21} are examined to further explore the influence of diene and dienophile substitution upon pentadienyl acrylate IMDA TS overlap repulsion and stereoselectivity (vide supra). We report the reactivities and *trans/cis*-stereoselectivities⁷ of IMDAs of terminally substituted pentadienyl acrylates (**2–5**), maleates (**6–10**), fumarates (**11–15**), crotonates (**16–17**), and chloroacrylates (**18–19**). To our knowledge, IMDA reactions of pentadienyl crotonates and chloroacrylates have not previously been reported in the literature.

Results and Discussion

IMDA Reactions. The IMDA precursors **1–19** were prepared by high-yielding esterification reactions between dienols and dienophile carboxylic acids and derivatives. Trienes **1–19** undergo IMDAs in 25–97% isolated yields in common aromatic solvents (Table 1). The cycloadducts are configurationally stable under the reaction conditions.

Cycloadduct stereochemistries were assigned on the basis of 2D NMR experiments. The stereochemistry of *trans*-fused, *exo*-IMDA adducts *trans*-**2P**, *trans*-fused C1-*i*-Pr adduct *trans*-**13P**, *Z*- and *E*-crotonate *exo*-cycloadducts *trans*-**16P** and *trans*-**17P**, and *cis*-fused, *endo*-IMDA adducts pentadienyl maleate *cis*-**6P** and *Z*-chloroacrylate *cis*-**18P** were confirmed by single-crystal X-ray analysis (Figure 2 and Supporting Information).

Relative Reactivities. Triene reactivity varies considerably with substitution, but the nature and orientation of the terminal dienophile (C9) substituent has a much greater influence upon the reaction rate than does the terminal diene (C1) substituent (see Table 1). For example, 9-*Z*-CO₂Me-substituted precursors **6–10** undergo complete conversion at 110 °C within 2–7 h, whereas 9-*E*-Me precursor **17** requires several weeks at

(13) (a) Paddon-Row, M. N.; Rondan, N. G.; Houk, K. N. *J. Am. Chem. Soc.* **1982**, *104*, 7162–7166. (b) Houk, K. N.; Rondan, N. G.; Wu, Y. D.; Metz, J. T.; Paddon-Row, M. N. *Tetrahedron* **1984**, *40*, 2257–2274. (c) Houk, K. N.; Paddon-Row, M. N.; Rondan, N. G.; Wu, Y. D.; Brown, F. K.; Spellmeyer, D. C.; Metz, J. T.; Li, Y.; Loncharich, R. J. *Science* **1986**, *231*, 1108–1117. (d) Li, Y.; Paddon-Row, M. N.; Houk, K. N. *J. Am. Chem. Soc.* **1988**, *110*, 3684–3686. (e) Paddon-Row, M. N.; Wong, S. S. *Chem. Phys. Lett.* **1990**, *167*, 432–438. (f) Paddon-Row, M. N.; Wong, S. S.; Jordan, K. D. *J. Chem. Soc., Perkin Trans. 2* **1990**, 417–423. (g) Paddon-Row, M. N.; Wong, S. S.; Jordan, K. D. *J. Am. Chem. Soc.* **1990**, *112*, 1710–1722. (h) Paddon-Row, M. N.; Wong, S. S.; Jordan, K. D. *J. Chem. Soc., Perkin Trans. 2* **1990**, 425–430. (i) Wong, S. S.; Paddon-Row, M. N. *J. Chem. Soc., Chem. Commun.* **1990**, 456–458. (j) Wong, S. S.; Paddon-Row, M. N.; Li, Y.; Houk, K. N. *J. Am. Chem. Soc.* **1990**, *112*, 8679–8686. (k) Wong, S. S.; Paddon-Row, M. N. *J. Chem. Soc., Chem. Commun.* **1991**, 327–330. (l) Wong, S. S.; Paddon-Row, M. N. *Aust. J. Chem.* **1991**, *44*, 765–770.

(14) Calculated Boltzmann product distributions (based upon the relative energies of respective TSs) and experimental product ratios (from kinetically controlled reactions) are generally in excellent agreement, and the computed TSs are used to rationalize the steric and electronic features that determine the experimental stereochemical IMDA outcomes.¹³ Finally, approaches are then devised to optimize the population of a targeted stereoisomeric product.

(15) For related investigations with pentadienyl acrylates, see: (a) White, J. D.; Nolen, E. G., Jr.; Miller, C. H. *J. Org. Chem.* **1986**, *51*, 1150–1152. (b) White, J. D.; Demnitz, F. W. J.; Oda, H.; Hassler, C.; Snyder, J. P. *Org. Lett.* **2000**, *2*, 3313–3316.

(16) These studies supported the total synthesis of the selective muscarinic receptor antagonist himbacine. See: (a) Wong, L. S.-M.; Sharp, L. A.; Xavier, N. M. C.; Turner, P.; Sherburn, M. S. *Org. Lett.* **2002**, *4*, 1955–1957. (b) Wong, L. S.-M.; Sherburn, M. S. *Org. Lett.* **2003**, *5*, 3603–3606. For a closely related approach to analogues of the natural product, see: (c) Van Cauwenberge, G.; Gao, L.-J.; Van Haver, D.; Milanese, M.; Viterbo, D.; De Clercq, P. *J. Org. Lett.* **2002**, *4*, 1579–1582. (d) Gao, L.-J.; Van Cauwenberge, G.; Hosten, N.; Van Haver, D.; Waelbroeck, M.; De Clercq, P. *J. ARKIVOC* **2003**, *iv*, 22–45.

(17) For seminal synthetic investigations with pentadienyl citraconate and mesaconate esters, see White, J. D.; Sheldon, B. G. *J. Org. Chem.* **1981**, *46*, 2273–2280.

(18) For synthetic studies on IMDA reactions of pentadienyl maleates and fumarates, see: (a) Burke, S. D.; Smith Strickland, S. M.; Powner, T. H. *J. Org. Chem.* **1983**, *48*, 454–459. (b) Jenkins, P. R.; Meneer, K. A.; Barraclough, P.; Nobbs, M. S. *J. Chem. Soc., Chem. Commun.* **1984**, 1423–1424. (c) Magnus, P.; Walker, C.; Jenkins, P. R.; Meneer, K. A. *Tetrahedron Lett.* **1986**, *27*, 651–654. (d) Eberle, M. K.; Weber, H. P. *J. Org. Chem.* **1988**, *53*, 231–235. (e) He, J. F.; Wu, Y. L. *Tetrahedron* **1988**, *44*, 1933–1940. (f) Batchelor, M. J.; Mellor, J. M. *J. Chem. Soc., Perkin Trans. 1* **1989**, 985–995. (g) Becher J.; Nielsen, H. C.; Jacobsen, J. P.; Simonsen, O.; Clausen, H. *J. Org. Chem.* **1988**, *53*, 1862–1871. (h) Toyota, M.; Wada, Y.; Fukumoto, K. *Heterocycles* **1993**, *35*, 111–114. (i) Berthon, L.; Tahri, A.; Uguen, D. *Tetrahedron Lett.* **1994**, *35*, 3937–3940. (j) Takatori, K.; Hasegawa, K.; Narai, S.; Kajiwar, M. *Heterocycles* **1996**, *42*, 525–528. (k) Arseniyadis, S.; Brondi-Alves, R.; Yashunsky, D. V.; Potier, P.; Toupet, L. *Tetrahedron* **1997**, *53*, 1003–1014.

(19) 1,3,8-Nonatriene numbering is retained for the esters described in this paper to facilitate comparisons with other IMDA precursors of the same general class.

(20) The bicyclic lactone cycloadducts derived from these triene precursors are common in nature and useful synthetic intermediates. For example, see: ref 18 and (a) Borzilleri, R. M.; Weinreb, S. M.; Parvez, M. *J. Am. Chem. Soc.* **1995**, *117*, 10905–10913. (b) Carter, R.; Hodgetts, K.; McKenna, J.; Magnus, P.; Wren, S. *Tetrahedron* **2000**, *56*, 4367–4382. (c) Toyota, M.; Yokota, M.; Ihara, M. *J. Am. Chem. Soc.* **2001**, *123*, 1856–1861.

(21) Cayzer, T. N.; Paddon-Row, M. N.; Sherburn, M. S. *Eur. J. Org. Chem.* **2003**, 4059–4068.

TABLE 1. C1- and C9-Substituted, Ester-Linked 1,3,8-Nonatriene (Scheme 1) Intramolecular Diels–Alder Reactions, with Reaction Temperatures (*T*), Times (*t*), Yields (*Y*), Experimental (exptl), Predicted (DFT) *trans*:*cis*-Product Ratios and *trans*:*cis*-Transition Structure Relative Energies (*E*_{Rel} kJ/mol) Showing *trans* (*t*) or *cis* (*c*) Preference

structure	C1-subst ^a	C9-subst ^a	<i>T</i> (°C)	<i>t</i> (h ^b)	<i>Y</i> (%)	<i>trans</i> : <i>cis</i> _{exptl} ^c	<i>trans</i> : <i>cis</i> _{DFT} ^d	<i>E</i> _{Rel}
1 ^d	H	H	180 ^e	190	56	30:70	38:62	<i>c</i> 1.88
2	Me	H	180 ^e	91	40	25:75	34:66	<i>c</i> 2.46
3	<i>i</i> -Pr	H	180 ^e	150	54	33:67	42:58 ^f	<i>c</i> 1.21
4	CO ₂ Me	H	180 ^e	60	85	44:56	50:50	<i>t</i> 0.75
5	BzO	H	180 ^e	79	61	26:74	24:76	<i>c</i> 4.36
6 ^g	H	<i>Z</i> -CO ₂ Me	110 ^h	4	97	83:17	94:6	<i>t</i> 8.85
7 ⁱ	Me	<i>Z</i> -CO ₂ Me	110 ^h	2	79	79:21	95:5	<i>t</i> 9.59
8	<i>i</i> -Pr	<i>Z</i> -CO ₂ Me	110 ^h	5	92	82:18	89:11 ^f	<i>t</i> 6.88
9	CO ₂ Me	<i>Z</i> -CO ₂ Me	110 ^h	7	86	78:22	92:8	<i>t</i> 7.73
10	BzO	<i>Z</i> -CO ₂ Me	110 ^h	6	75	60:40	82:18	<i>t</i> 4.94
11 ^j	H	<i>E</i> -CO ₂ Me	110 ^h	205	77	58:42	55:45	<i>t</i> 0.71
12 ⁱ	Me	<i>E</i> -CO ₂ Me	110 ^h	23	85	65:35	59:41	<i>t</i> 0.85
13	<i>i</i> -Pr	<i>E</i> -CO ₂ Me	110 ^h	162	88	68:32	68:14 ^f	<i>t</i> 5.75
14 ⁱ	CO ₂ Me	<i>E</i> -CO ₂ Me	110 ^h	107	90	83:17	78:22	<i>t</i> 5.67
15 ^g	BzO	<i>E</i> -CO ₂ Me	110 ^h	45	63	78:22	82:18	<i>t</i> 5.60
16	Me	<i>Z</i> -Me	220 ^h	21	54	52:48	60:40	<i>t</i> 1.58
17	Me	<i>E</i> -Me	220 ^h	47	25	34:66	35:65	<i>c</i> 2.30
18	Me	<i>Z</i> -Cl	180 ^h	40	61	82:18	90:10	<i>t</i> 7.60
19	Me	<i>E</i> -Cl	180 ^h	187	38	28:72	15:85	<i>c</i> 5.59

^a Abbreviations: Me = methyl; *i*-Pr = isopropyl; BzO = benzoyloxy; and CO₂Me = carbomethoxy. ^b Time taken for >95% conversion of starting triene. ^c The mean of the ratios measured from GC of the crude reaction mixture, ¹H NMR of the crude reaction mixture, and the isolated yields after purification. The difference between the three sets of ratios was at most ±5%. ^d Result taken from ref 21. ^e 1,2-Dichlorobenzene. ^f Note, the *i*-Pr and *t*-Bu groups were employed during experiments and DFT studies, respectively. ^g Previously reported to give *exo*-cycloadduct *trans*-**15** exclusively in refluxing xylenes^{18g} or 1,2-dichlorobenzene at 110 °C.¹⁸ⁱ ^h Toluene. ⁱ Result taken from refs 8 and 11. ^j Previously reported to give a *trans*:*cis* ratio of 2:1.^{18f}

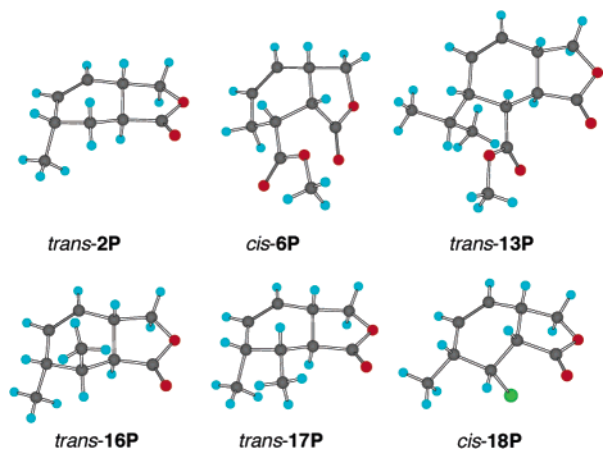


FIGURE 2. IMDA product molecular structures from single-crystal X-ray analyses.

180 °C. The 9-substituent reactivity order (reaction temperature in brackets) is *Z*-CO₂Me (110 °C) > *E*-CO₂-Me (110 °C) ≫ *Z*-Cl (180 °C) > *Z*-Me (180 °C) ≈ H (180 °C) > *E*-Cl (180–220 °C) > *E*-Me (180–220 °C). Thus, 9-*Z*-substituents do not impact unfavorably upon the reaction rate, whereas 9-*E*-substituents do. This general trend is evidently overridden, however, by the presence of the dienophile “activating” carbomethoxy group, which promotes a significant rate enhancement. A 9-chlorine leads to a much more modest, yet still significant, rate acceleration.

In contrast, the C1-substituent (Me, *i*-Pr, CO₂Me or OBz) does not markedly affect the temperature required for cyclization, with the reactivity order of C1-substituted systems principally dependent on the dienophile. This result is seemingly at odds with earlier findings.²² Interestingly, the acrylate derivative of the electron poor C1-CO₂Me diene **4** undergoes a more facile IMDA (60 h) than all other acrylates studied, including the electron rich C1-benzoyloxy system **5** (79 h). Maleate derivatives of C1 ester-**9** and C1 benzoyloxy-**10** dienes underwent IMDAs with similar ease. Evidently, assumptions relating to the expected rate-enhancing/rate-retarding influence of electron donors/acceptors attached to the diene terminus are not valid for IMDAs of this type.

Stereoselectivities. With few exceptions, the nature and orientation of the terminal dienophile (C9) substituent has a much greater influence upon the product stereoselectivity than does the terminal diene (C1) substituent. Thus, the IMDA for the parent system, **1**, shows fairly strong *cis*-selectivity (**1**, Table 1) and comparable *cis*-selectivity is displayed for the C1-substituted systems (**2–5**). *E*-9-substitution with methyl and chloro substituents likewise displayed predominant *cis*-selectivity (**17** and **19**). In contrast, the IMDA of the “parent” fumarate system (**11**) slightly favored *trans*-selectivity. Preference for the *trans*-isomer in the fumarate series is progressively strengthened by C1-substitution in the order H <

(22) (a) Wu, T.-C.; Houk, K. N. *Tetrahedron Lett.* **1985**, 26, 2293–2296. (b) Robiette, R.; Marchand-Brynaert, J.; Peeters, D. *J. Org. Chem.* **2002**, 67, 6823–6826.

Me < *i*-Pr < OBz < CO₂Me (**11–15**). *Z*-9-Methyl substitution (**16**) gave a ca. 50:50 *cis*:*trans* mixture, whereas the *Z*-9-chloro- (**18**) and maleate precursors (**6–10**) gave moderate to high *trans*-selectivity, irrespective of the steric size or the electronic makeup of the diene C1 substituent.

Computational Studies. To gain mechanistic insight into the origins of the experimentally observed IMDA reactivities and stereoselectivities, gas-phase DFT calculations—specifically, B3LYP/6-31+G(d)—have been carried out to locate the IMDA TSs for a broad range of substituted penta-1,3-dienyl acrylates. The results of this extended study form the subject of ongoing investigations.²³ Herein, we restrict discussion to three issues: (1) the geometrical features of the TSs, (2) the reason behind the lower reactivity of *E*-9-substituted acrylates, compared to their *Z* stereoisomers, and (3) the origin of *cis*/*trans*-stereoselectivity in the parent pentadienyl acrylate **1**.

The computed *trans*/*cis*-product ratios are presented in Table 1. Overall, there is good agreement with the experimental data. Particularly striking is the finding that the calculated ratios reflect the subtle changes brought about by various C1-substituents (cf. **1**, **2**, **4**, and **5**; cf. **6**, **7**, **9**, and **10**; cf. **11**, **12**, **14**, and **15**). It is emphasized that the computed stereoselectivities refer to gas-phase IMDAs, whereas the experimental reactions were carried out in solvent. Preliminary calculations indicate that the inclusion of solvent effects, in the form of a polarization continuum model (PCM),^{24–26} leads to a moderately improved agreement with experiment. For example, the PCM-B3LYP/6-31+G(d) stereoselectivity for the IMDA of C1-Me-C9-*Z*-CO₂Me maleate **7** is 88:12 (toluene; $\epsilon = 2.379$), mid-way between the experimental (79:21; toluene) and computed gas-phase (95:5; B3LYP/6-31+G(d)) selectivities.

Transition Structure Geometries. Referring to Figure 3, there are six significant geometrical parameters associated with the IMDA TS. These are: the peripheral and internal forming bonds; r_p and r_i , respectively, the bond forming asynchronicity, Δr_{as} ($= |r_p - r_i|$); the twist-mode asynchronicity dihedral angle, θ_{as} (the dihedral angle C1–C4–C8–C9); the dihedral angle, θ_1 , made between the carbonyl group and the dienophile double bond; and, finally, the dihedral angle, θ_2 , which gives the degree of twisting about the C4–C8 internuclear axis in the forming γ -butyrolactone ring. Two other dihedral angles, namely θ_3 and θ_4 are important parameters when considering the origin of *cis*/*trans*-stereoselectivity in the

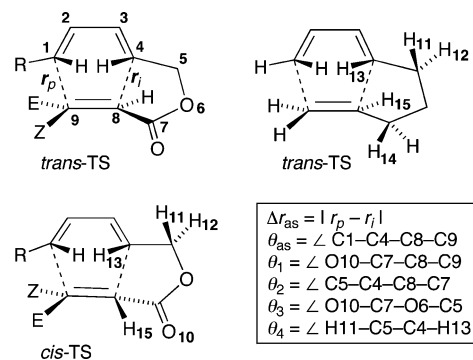


FIGURE 3. Schematic of IMDA transition structures (*cis* or *trans*, CH₂OC(=O), and CH₂CH₂CH₂-tethered) depicting the numbering schemes and relevant geometrical parameters.

IMDA reaction of **1** (vide infra). Values for parameters θ_{as} , θ_1 and θ_2 for selected TSs are given in Table 2.

In all TSs, the peripheral bond is longer than the internal bond, although the bond-forming asynchronicity in the *trans*- and *cis*-IMDA TSs for the parent system, **1**, is insignificant (Figure 4). These trends are depicted graphically in Figure 5. The two Figure 5 plots are strikingly similar, demonstrating that a triene substituent has a very similar influence on both the *cis*- and *trans*-TSs. The magnitude of the bond-forming asynchronicity, Δr_{as} , is much more sensitive to substitution at C9 than at C1 and increases along the series 9-Me < 9-Cl < 9-CO₂Me, reaching a maximum value of 0.84 Å in the *trans*-IMDA TS for the 1-Me-*Z*-9-CO₂Me molecule **7**. This high degree of bond-forming asynchronicity, induced by substitution on the dienophile with an activating group, such as ester or aldehyde, has been noted for other Diels–Alder reactions, both intermolecular and intramolecular.^{28–32} We note that whereas there exists a general correlation between the magnitude of Δr_{as} (Figure 5) and reactivity (Table 1), there is no clear correlation between Δr_{as} and stereoselectivity.

In general, Δr_{as} is slightly larger for *trans*-TSs than for the corresponding *cis*-congeners. Even though Δr_{as} varies significantly throughout the series of TSs studied, the sum of the internal and peripheral bond lengths remains approximately constant (ca. 4.5–4.6 Å). Thus, any increase in the length of the developing peripheral bond is compensated by contraction of the forming internal bond, thereby maintaining as much bond-forming stabilization energy as possible. Consistent with their small influence on the experimental reaction rates and stereoselectivities, C1-substituents lead to smaller TS geometric changes than 9-substituents (cf. *trans*-C1-methyl ($r_1 = 2.360$ Å; $r_2 = 2.127$ Å) and *trans*-9-methyl ($r_1 = 2.429$ Å; $r_2 = 2.090$ Å). Furthermore, for a specific 9-substituent, the *Z*-dienophile TS is slightly more asynchronous than the *E*-dienophile TS.

From their computational studies of the IMDAs of 1,3,8-nonatriene (Figure 1A), Houk et al. identified an

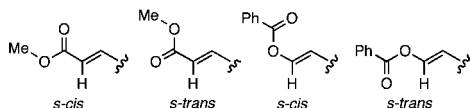
(23) Paddon-Row, M. N.; Moran, D.; Jones, G. A.; Sherburn, M. S. Manuscript in preparation.

(24) Cossi, M.; Rega, N.; Scalmani, G.; Barone, V. *J. Comput. Chem.* **2003**, *24*, 669–681.

(25) Cammi, R.; Mennucci, B.; Tomasi, J. *J. Phys. Chem. A* **2000**, *104*, 5631–5637.

(26) Miertus, S.; Scrocco, E.; Tomasi, J. *Chem. Phys.* **1981**, *55*, 117–129.

(27) The *s-cis* and *s-trans* isomers of carbomethoxy and benzoyloxy groups:



(28) Kong, S.; Evanseck, J. D. *J. Am. Chem. Soc.* **2000**, *122*, 10418–10427.

(29) Houk, K. N.; Gonzalez, J.; Li, Y. *Acc. Chem. Res.* **1995**, *28*, 81–90.

(30) Singleton, D. A.; Merrigan, S. R.; Beno, B. R.; Houk, K. N. *Tetrahedron Lett.* **1999**, *40*, 5817–5821.

(31) Gajewski, J. J.; Peterson, K. B.; Kagel, J. R.; Huang, Y. C. *J. Am. Chem. Soc.* **1989**, *111*, 9078–9081.

(32) Tolbert, L. M.; Ali, M. B. *J. Am. Chem. Soc.* **1984**, *106*, 3806–3810.

TABLE 2. Salient Dihedral Angles (See Figure 3) of B3LYP/6-31+G(d)-Optimized IMDA TSs^a

TS	C1-subst	C9-subst	trans- θ_{as}°	cis- θ_{as}°	trans- θ_1°	cis- θ_1°	trans- θ_2°	cis- θ_2°
1	H	H	-8.8	5.9	31.0	-31.0	44.7	-42.0
2	Me	H	-8.8	5.9	31.0	-31.4	44.4	-41.2
3	<i>t</i> -Bu	H	-10.0	5.5	30.7	-30.3	43.3	-41.2
4	CO ₂ Me	H	-10.0	5.5	31.3	-30.5	43.4	-41.7
5	BzO	H	-10.3	5.9	32.9	-31.6	42.9	-41.3
6	H	Z-CO ₂ Me	-21.2	15.6	45.4	-45.3	31.6	-28.2
7	Me	Z-CO ₂ Me	-22.0	16.5	45.5	-45.0	31.0	-27.2
8	<i>t</i> -Bu	Z-CO ₂ Me	-28.5	18.7	45.6	-44.0	27.5	-26.5
9	CO ₂ Me	Z-CO ₂ Me	-22.0	13.2	44.9	-44.2	31.6	-29.3
10	BzO	Z-CO ₂ Me	-23.0	16.2	46.2	-45.0	30.4	-27.6
11	H	<i>E</i> -CO ₂ Me	-9.6	4.0	30.7	-28.9	42.3	-41.2
12	Me	<i>E</i> -CO ₂ Me	-11.0	3.0	30.4	-27.4	40.9	-40.5
13	<i>t</i> -Bu	<i>E</i> -CO ₂ Me	-9.2	2.4	28.0	-25.4	41.0	-40.5
14	BzO	<i>E</i> -CO ₂ Me	-7.8	2.7	29.7	-27.5	42.3	-41.3
15	CO ₂ Me	<i>E</i> -CO ₂ Me	-11.3	1.4	31.8	-27.8	40.6	-41.3
16	Me	Z-Me	-16.0	11.7	35.6	-36.0	37.3	-34.2
17	Me	<i>E</i> -Me	-5.3	1.3	26.8	-26.2	45.4	-42.6
18	Me	Z-Cl	-21.7	17.7	43.3	-44.3	30.5	-25.9
19	Me	<i>E</i> -Cl	-5.4	1.7	27.8	-27.3	45.9	-43.2

^a Only the most stable *s-cis*-CO₂Me and *s-trans*-BzO substituent conformations²⁷ are included. See the Supporting Information for details of the alternate conformations.

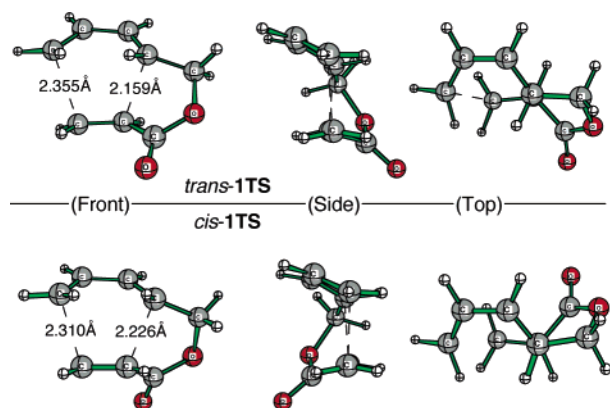


FIGURE 4. Optimized trans- and cis-TS structures of the unsubstituted parent, **1** (Top: view down developing C4–C8 bond).

important form of asynchronicity in the TSs which they called twist-mode asynchronicity,^{5,6} which arises from twisting of the dienophile about the C4–C8 internuclear axis and is expressed by θ_{as} (Figure 3). The presence of this type of asynchronicity in IMDA TSs—which is absent in symmetrical TSs, such as that between butadiene and ethane (i.e. $\theta_{as} = 0^\circ$)—is caused by the need to reduce strain in the developing tether-containing ring. A degree of twist-mode asynchronicity is found to exist in the trans- and cis-TSs for the parent system **1**, amounting to a twist of -9° in the exo-direction, in the case of the trans-TS, and to a twist of 6° in the endo-direction, in the case of the cis-TS. Whereas the most obvious structural manifestation of twist-mode asynchronicity is θ_{as} , the twisting of the dienophile with respect to the diene, its *cause* is the reduction of strain in the tether-containing ring, which is quantified by θ_2 . The close relationship between θ_{as} and θ_2 is revealed in Figure 6, whereas the values of θ_{as} and θ_2 for a particular TS differ, and a change in one parameter is reflected in the other. Importantly, model structures allow the calculation of the lowest energy value for θ_2 for a particular tether, information not readily accessible by consideration of θ_{as} (vide infra).

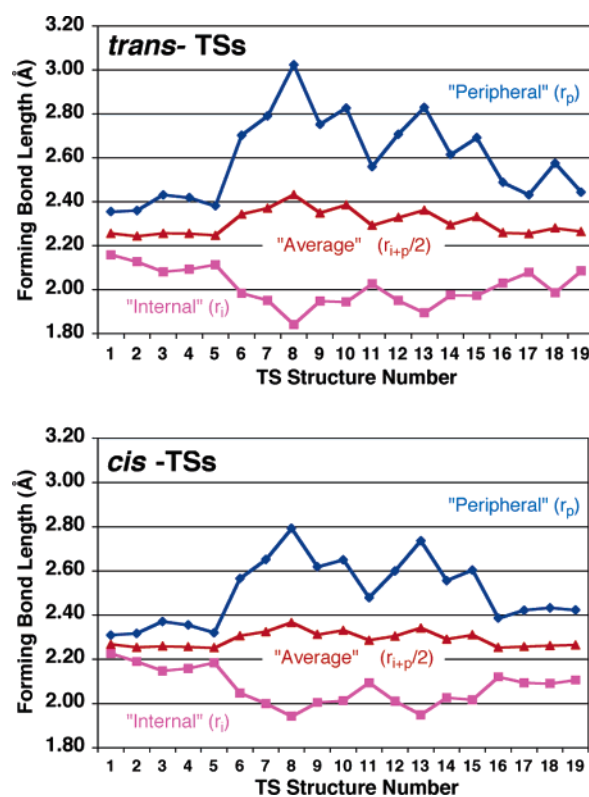


FIGURE 5. Graphical summary of peripheral (r_p) and internal (r_i) forming bond lengths (Å) for trans- and cis-TSs (Figure 3). The degree of bond-forming asynchronicity, Δr_{as} , is given by the separation between the blue and pink data lines; the greater the separation, the stronger the asynchronicity (e.g., *trans*-**14**TS, C9-*E*-CO₂Me, $\Delta r_{as} = 0.534$ Å; Table 2).

The forming five-membered γ -butyrolactone ring is not planar in any of the IMDA TSs, as exemplified by the trans- and cis-parent TSs for which θ_2 is 45° and -42° , respectively (Figure 4). The magnitude of θ_2 varies only slightly with C1-substitution or *E*-9-substitution but is markedly diminished, by as much as 15° , by Z-9-substitution (Figure 6). For example, $\theta_2 = 28^\circ$, 30° , 37° , and 31° for the trans-TSs associated with **8**, **10**, **16**

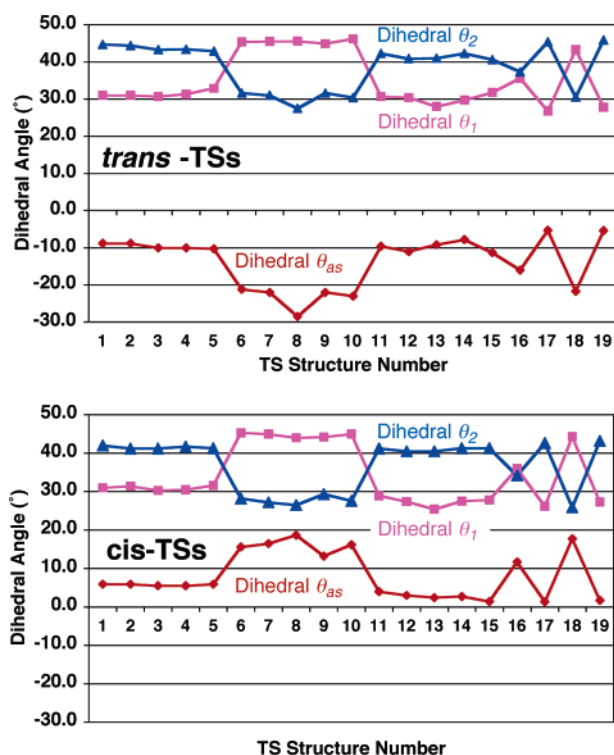


FIGURE 6. Plots summarizing the *trans*- and *cis*-TS (Figure 3) twist-mode asynchronicity (θ_{as}), the dihedral angle between the carbonyl group and the dienophile double bond (θ_1), and the forming γ -butyrolactone ring C4–C8 internuclear axis dihedral angle (θ_2).

and **18**, respectively. Similar numerical values of θ_2 are found for the corresponding *cis*-series of TSs.

The optimal value for θ_2 in the forming γ -butyrolactone ring in the *trans*- and *cis*-TSs was estimated at ca. -38° and 42° for the *cis*- and *trans*-TSs, respectively (see Supporting Information). If twist-mode asynchronicity were, somehow, prevented from taking place in the TSs, then molecular (i.e. Dreiding) models suggest that θ_2 would be about 60° in the *trans*- and *cis*-TSs, representing a twist angle strain of ca. 18 – 22° in both TSs. This strain is ameliorated in the real TSs by twist-mode asynchronicity which reduces θ_2 by twisting in the exo- and endo-directions in the respective *trans*- and *cis*-TSs.

While we find that the magnitude of θ_{as} is little affected by 9-*E*-substituents, its numerical value is substantially increased by 9-*Z*-substituents. For example, $\theta_{as} \approx -22^\circ$ in the *trans*-TSs for both **6** (9-*Z*-CO₂Me) and **18** (9-*Z*-Cl), and is only slightly smaller ($\approx 18^\circ$) for the *cis*-TSs.

The comparatively strong influence of 9-*Z* substituents on the magnitudes of θ_2 and θ_{as} may be traced to a combination of steric and electrostatic repulsion between the *Z*-substituent and the carbonyl oxygen atom of the tether (O10 in Figure 3). For all IMDA TSs possessing the methylenoxycarbonyl tether, the carbonyl group of the tether is substantially twisted out of the plane of the dienophile double bond, pointing away from the diene face (Figure 4). In the case of both *trans*- and *cis*-IMDA TSs for the parent molecule **1**, the numerical value of θ_1 is 31° and this value is only slightly smaller (ca. 27°) for 9-*E*-substituted TSs. In marked contrast, 9-*Z*-substituents cause θ_1 to increase, often by substantial amounts

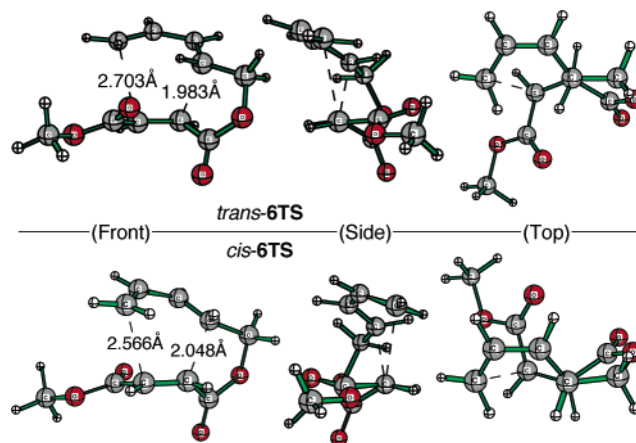


FIGURE 7. Optimized *trans*- and *cis*-TS structures of C9–CO₂Me maleate, **6** (Top = view down developing C4–C8 bond).

($\approx 13^\circ$). For example, the numerical value of θ_1 is approximately 44° for the *trans*- and *cis*-TSs of 9-*Z*-Cl and 9-*Z*-CO₂Me; the 9-*Z*-Me substituent has a smaller influence ($\theta_1 \approx 36^\circ$).

The 9-*Z*-substituent-induced increase in the value of θ_1 has the geometrical consequence of reducing the magnitude of θ_2 , and this, in turn, causes twisting of the dienophile double bond about the C4–C8 internuclear axis, thereby modulating the magnitude of the twist-mode asynchronicity angle θ_{as} . This twisting occurs in the exo direction, in the case of *trans*-TSs, and in the endo-direction in the case of *cis*-TSs, as is clearly evident from comparison of the *trans*- and *cis*-TSs for the parent system **1** (Figure 4) with those for the 9-*Z*-CO₂Me system **6** (Figure 7). The mutually dependent nature of θ_1 , θ_2 , and θ_{as} is clearly evident on inspection of Figure 6.

Reactivity of *E*-9-Systems Compared to *Z*-9-Systems. As mentioned above, qualitative experimental observations indicated that the 9-*E*-substituted systems are less reactive than their 9-*Z*-stereoisomers. Preliminary kinetic studies on the IMDA reactions of 1-Me-9-*E*-CO₂Me fumarate, **12**, and 1-Me-9-*Z*-CO₂Me maleate, **7**, in benzene solvent confirm the reactivity differences. The experimental activation energies for the reactions of **7** and **12**, leading to *trans* products,³³ are 81 and 90 kJ/mol, respectively, thereby revealing that the activation energy for the 9-*Z*-CO₂Me stereoisomer is ca. 9 kJ/mol lower than that for the 9-*E*-CO₂Me stereoisomer. This is an unexpected result, since it is well-known that

(33) The kinetic data are not yet precise enough to obtain separate activation energies for each of the IMDA reactions leading to *cis* and *trans* products. Instead, the Arrhenius plot used the logarithm of the sum of the rate constant for *cis* and *trans* reactions vs $1/T$, thereby producing an activation energy that is a weighted average of those for each of the *cis* and *trans* reactions. Because the major product from the IMDA reaction of both **7** and **12** is the *trans* stereoisomer, the activation energy resembles more that for formation of the *trans* product than for the *cis* product.

(34) (a) Sauer, J.; Wiest, H.; Mielert, A. *Z. Naturforsch.* **1962**, *17b*, 203–204. (b) Sauer, J.; Lang, D.; Wiest, H.; *Z. Naturforsch.* **1962**, *17b*, 206. (c) Huisgen, R. *Angew. Chem., Int. Ed. Engl.* **1963**, *2*, 633–645. (d) Zutterman, F.; Kreif, A. *J. Org. Chem.* **1983**, *48*, 1135–1137. (e) Grieco, P. A.; Yoshida, K.; He, Z. *Tetrahedron Lett.* **1984**, *25*, 5715–5718. (f) Singleton, D. A.; Schulmeier, B. E.; Hang, C.; Thomas, A. A.; Leung, S.-W.; Merrigan, S. R. *Tetrahedron* **2001**, *57*, 5149–5160. (g) Akakura, M.; Koga, N. *Bull. Chem. Soc. Jpn.* **2002**, *75*, 1785–1793.

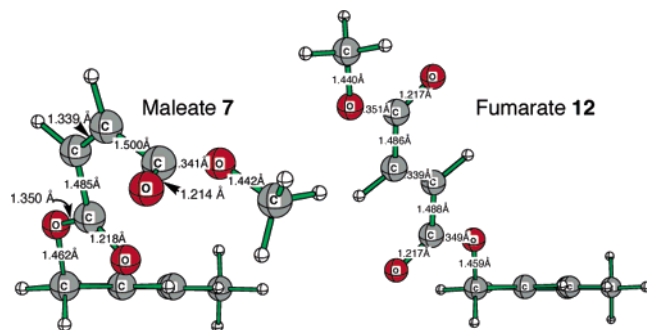


FIGURE 8. Optimized reactant structures of the maleate, **7**, and the fumarate, **12**.

E-dienophiles are significantly more reactive than *Z*-dienophiles in intermolecular cycloadditions.³⁴

The B3LYP/6-31+G(d) gas-phase activation energies for **12** and **7**—calculated by subtracting the thermally corrected (383 K) energy of the reactant from that of the corresponding TS (reactant geometries are shown in Figure 8)—are 136.1 and 116.6 kJ/mol for the trans reactions for **12** and **7**, respectively, and 137.0 and 126.2 kJ/mol for the cis reactions for **12** and **7**, respectively. While correctly predicting a higher activation energy for the IMDA reaction of **12**, compared to **7**—by 20 and 11 kJ/mol for the trans and cis pathways, respectively—the computed activation energies are substantially higher than the experimental ones, by as much as 46 kJ/mol. This serious discrepancy between the computed and experimental activation energies is surprising, considering that the B3LYP functional is reported to give activation energies for intermolecular Diels–Alder reactions that are in excellent agreement (to within 4 kJ/mol) with experiment.^{28,35,36}

The computed IMDA activation energies for *E* and *Z* 1,9-dimethylacrylates, **16** and **17**, and 1-methyl-9-chloroacrylates, **18** and **19**, are also suspiciously high (Figure 9, Table 1), although experimental values are not yet available. Notwithstanding the overestimated activation barriers, the B3LYP/6-31+G(d) level correctly predicts higher IMDA activation energies for the *E* stereoisomers, compared to the respective *Z* stereoisomers. Significantly, the origin of this behavior does not seem to be electronic, because it is observed for 9-substituents possessing quite different electronic characteristics (i.e., CO₂Me, Cl, Me).

Inspection of Figure 9 reveals that, for a given substituent, the 9-*E* stereoisomer is more stable than the 9-*Z* stereoisomer in both reactants and TSs, and that this

(35) Wiest, O.; Houk, K. N. In *Topics in Current Chemistry*; Nalewajski, R. F., Ed.; Springer-Verlag: Berlin, 1996; Vol. 183, pp 1–24.

(36) Inclusion of nonspecific solvent effects (PCM) and using the 6-31G(d) basis set instead of the 6-31+G(d) basis set reduces the discrepancy between theory and experiment (full geometry optimizations were carried out at all levels). Using the 6-31G(d) basis set gives the following (thermally corrected 383 K) activation energies (kJ/mol): 101 (*Z*) and 123 (*E*) for the trans pathway and 112 (*Z*) and 124 (*E*) for the cis pathway. Inclusion of benzene solvation (B3LYP/6-31G(d)-PCM) gave the following (thermally corrected 383 K) activation energies: 97 and 117 for the trans pathway, and 105 (*Z*) and 119 (*E*) for the cis pathway. The computed trans activation energies for the *Z* (97 kJ/mol) and the *E* (119 kJ/mol) are, respectively, 17 and 27 kJ/mol higher than the respective experimental quantities. Although an improvement, the B3LYP/6-31G(d)-PCM activation energies remain unacceptably high. This problem is being further investigated.

relative stability of the *E* stereoisomer is much greater in the reactants than in the IMDA TSs. For example, **12** is 26 kJ/mol more stable than **7**, but this stability is reduced to only 6 kJ/mol in the corresponding trans TSs.

This trend may be plausibly explained in terms of strain and conjugation effects in the reactants. For the reactants, the 9-*Z* stereoisomer is less stable than the 9-*E* isomer because of the presence of steric and electrostatic (dipole–dipole) repulsions between the substituent and the tether carbonyl group in the former isomer, which are obviously absent in the latter. For example, the aforementioned electrostatic repulsion is sufficiently strong in the 9-*Z*-ester reactant **7** to cause out-of-plane twisting of either the substituent group or the tether carbonyl group by about 67° (Figure 8). In the 9-*E* reactant, **12**, both carbonyl groups lie in the plane of the C8=C9 double bond. Although our calculations predict that the tether carbonyl group remains in the plane of C8=C9 in the 9-*Z*-Me, **16**, and 9-*Z*-Cl, **18**, reactants, strain is present in these molecules. Thus, **16** is 10 kJ/mol less stable than the 9-*E*-Me isomer, **17**, due mainly to steric effects, and **18** is even less stable than the corresponding *E* stereoisomer, **19**, by 16 kJ/mol, probably due to the presence of electrostatic effects, in addition to steric repulsion.

In contrast to the reactant geometries, those for the IMDA TSs are distinguished by marked noncoplanarity of the tether carbonyl group with the C8=C9 double bond, the magnitude of which is given by θ_1 . For the 9-*E*-substituted TSs it is about 30°, and for the 9-*Z*-substituted TSs it is about 40°. In addition, the C8 carbon atom displays a significant degree of pyramidalization in all IMDA TSs, as measured by the dihedral angle C7–C8–C9–H15, which ranges from 140° to 150° (this angle for a perfectly pyramidalized sp³ atom is 120°). These two geometrical features of the IMDA TSs lead to a significant decrease in the degree of conjugation between the tether carbonyl group and the C8=C9 double bond in the TSs, compared to the 9-*E*-substituted reactant in which the conjugation is fully operational in a strain-free environment. Although this type of conjugation is also weak in the IMDA TSs for the 9-*Z*-substituted stereoisomers, this energy penalty is offset by a concomitant reduction in the steric and electrostatic strain effects in the TSs—compared to the respective 9-*Z*-substituted reactants—a result caused by the out-of-plane twisting of the tether carbonyl group, thereby increasing the distance between the 9-*Z*-substituent and the tether carbonyl oxygen atom.³⁷

Thus, the enhanced reactivity of the 9-*Z*-substituted systems compared to their 9-*E*-substituted isomers is explained. In the case of intermolecular Diels–Alder reactions, *E*-dienophiles are no longer obliged to suffer out-of-plane twisting of the substituents, with concomitant loss of some delocalization energy, although the substituents in the *Z*-dienophiles remain twisted out-of-plane in the TS, thereby incurring an energy penalty due

(37) For the 9-*Z*-ester reactant, **7**, the tether carbonyl group is already twisted out-of-plane ($\theta_1 \approx 70^\circ$) and so little, if any, conjugation exists between the tether carbonyl group and the C8=C9 double bond. It is this reduced effect of conjugation in the reactant, **7**, rather than diminished steric and electrostatic interactions between the 9-*Z*-CO₂-Me substituent and the tether carbonyl group, which is responsible for the smaller activation energy for 9-*Z*-ester, **7**, compared to the 9-*E*-stereoisomer, **12**.

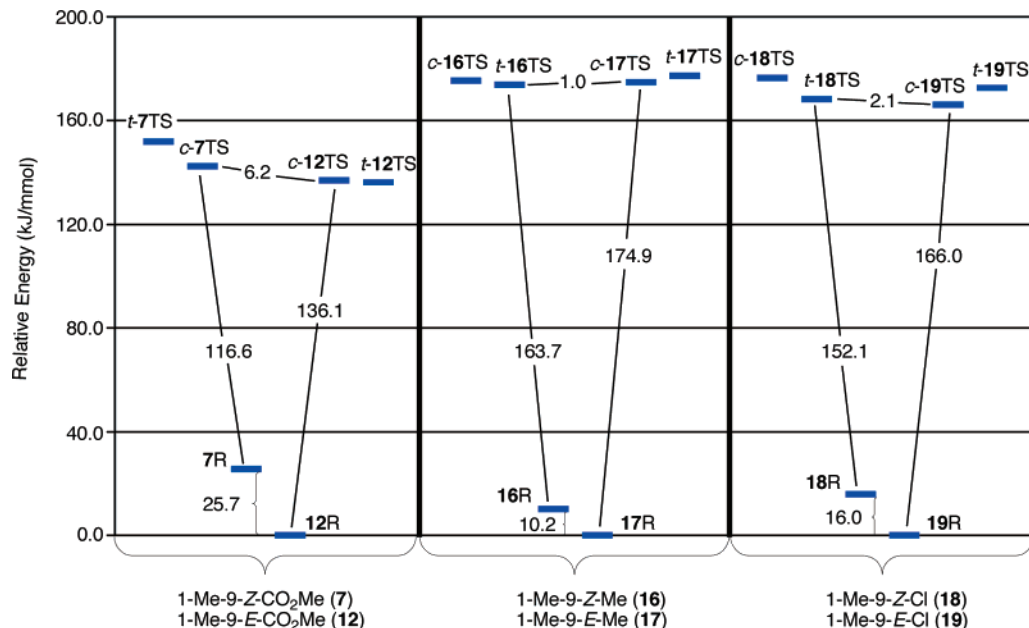


FIGURE 9. Energy diagrams for *E*- and *Z*-1-Me-9- CO_2Me , **7** and **12**, 1,9-dimethyl, **16**, **17**, and 1-Me-9-Cl, **18**, **19**, reactants (R) and their *cis* (*c*) and *trans* (*t*) IMDA TSs (TS). Only the smaller activation energy (kJ/mol, including ZPVE corrections), corresponding to either *cis*- or *trans*-TS, is depicted for each stereoisomer (*E* or *Z*); the higher activation energy for each stereoisomer may be readily calculated from the data given in both this Figure and Table 1. The energetically most stable reactant geometries were employed throughout.

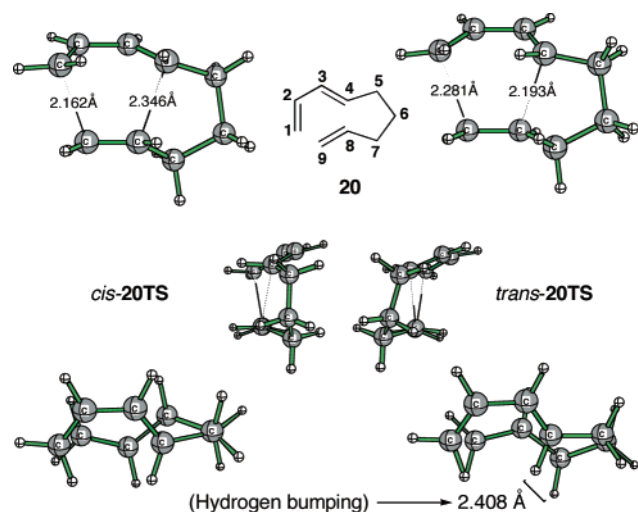


FIGURE 10. *Cis*- and *trans*-TSs for the IMDA reaction of **20**.

to steric congestion between the substituents and the approaching diene. It is, therefore, not surprising that *E*-dienophiles are significantly more reactive than *Z*-dienophiles in *intermolecular* cycloadditions.³⁴

Origin of *cis/trans* Selectivity in IMDA Reaction of Ester-Tethered 1,3,8-Nonatriene **1.** It is instructive to consider the stereoselectivity of the IMDA reaction of 1,3,8-nonatriene **20** (Figure 10).

Experimentally, as found for the corresponding acrylate **1**, the IMDA reaction of **20** is *cis*-selective, giving a 70:30 ratio of *cis*:*trans* products, which was reproduced computationally by Houk et al., using HF/3-21G.⁵ Our DFT calculations also predict *cis*-selectivity, favoring *cis*-**20TS** over *trans*-**20TS** by 5.85 kJ/mol.

Houk et al. attributed the *cis*-selectivity in this reaction to the presence of an adverse steric interaction between H13 and H14 in the *trans* TS—they are 2.41 Å apart—which is absent in the corresponding *cis* TS (see Figure 3 for numbering scheme).^{4,5} In addition, *trans*-**20TS** experiences more torsional strain about the C5–C6 bond than does *cis*-**20TS**; the dihedral angles between the C5H and C6H bonds are ca. 17° in the former, compared to ca. 36° in the latter TS. These two unfavorable features in *trans*-**20TS** are evidently more energetically costly than the close contact between H13 and H15 in *cis*-**20TS** (2.35 Å).

The *cis*-selectivity of 1.9 kJ/mol for the IMDA reaction of acrylate **1** is weaker than that for **20**. Unlike *trans*-**20TS**, however, there is no significant transannular strain between the C4 and C7 groups in *trans*-**1TS**; H13 is 2.57 and 3.41 Å from C7 and O10, respectively, with the former distance being slightly larger than the sum of the van der Waals radii of a hydrogen and a carbon atom. Possible differences in conjugation in the *cis*- and *trans*-IMDA TSs for **1** cannot be responsible for the observed *cis*-selectivity because the dihedral angle, θ_1 (see Figure 3 for definitions of dihedral angles θ), between the carbonyl group and the dienophile bond is the same (31°) in both TSs. Likewise, the torsional angle about the O6–C7 bond is comparable (ca. 162°) in both TSs.

The only obvious difference in strain in the *cis*- and *trans*-IMDA TSs for **1** that we were able to identify is the presence of torsional strain in *cis*-**1TS**; in this TS, the conformation about the C4–C5 bond is unfavorably C–H/C–H eclipsed²⁵ with a 3.3° dihedral angle, θ_4 , between the C5–H11 and C4–H13 bonds (Figure 11).

In contrast, the C4–C5 bond in *trans*-**1TS** adopts the favored C–H/C–H staggered²⁵ conformation, with $\theta_4 \approx 64^\circ$ (Table 1). Using pentadienyl formate **21** as a model

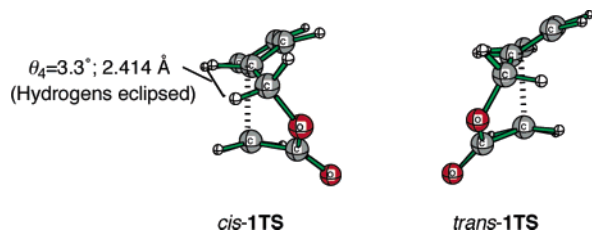


FIGURE 11. Cis- and trans-TSs for the IMDA reaction of **1**.

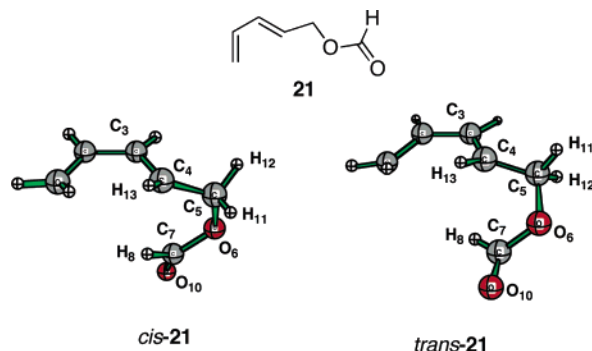


FIGURE 12. Models used to estimate the difference in the torsional strain about the C4–C5 bond in the cis- and trans-TSs of **21**.

for estimating torsional strain in *cis*- and *trans*-**1TS** (Figure 12), the staggered conformation in *trans*-**1TS** is estimated to be ca. 2.5 kJ/mol more stable than the eclipsed conformation in *cis*-**1TS**. Note that this model also takes into account repulsive interactions between C4 and C7 which are slightly larger in *trans*-**1TS** (C4–C7 separation 2.56 Å; C7–H13 separation 2.56 Å) than in *cis*-**1TS** (C4–C7 separation 2.61 Å; C7–H13 separation 3.29 Å).

The reason the C4–C5 bond has an eclipsed conformation in *cis*-**1TS**, whereas it is staggered in *trans*-**1TS** is due to the resistance of an ester group to out-of-plane twisting about the alkoxy bond. Achievement of a staggered conformation about the C4–C5 bond in *cis*-**1TS** would require the TS dihedral angle θ_3 to be reduced from 162° to ca. 100°, and this is energetically too costly. *cis*-**20TS** is free of C4–C5 torsional strain because of the more flexible nature of the trimethylene tether.

Combining the overall energetic preference of ca. 1.9 kJ/mol for *cis*-**1TS**, relative to *trans*-**1TS**, with the former's unfavorable C4–C5 torsional strain energy of ca. 2.5 kJ/mol suggests the presence of an additional, stabilizing, factor in *cis*-**1TS**, amounting to ca. 4.5 kJ/mol. We postulate that this factor is a stabilizing interaction between the diene and the tether carbonyl group which occupies an endo disposition with respect to the diene moiety. This stabilizing interaction could be due to a combination of secondary orbital interactions,^{26,27} perhaps of the Singleton kind, between C4 and C7,²⁸ and electrostatic interactions between the diene and carbonyl groups.²⁹

Conclusion

Substituted pentadienyl acrylates were shown to undergo synthetically useful IMDA reactions and many

experimental observations pertaining to reactivity and stereoselectivity were explained by interpretation of computed TSs. Several facets of the present study are noteworthy. First, *Z*-dienophiles were shown to be more reactive than their *E*-substituted congeners—a reversal in the order of reactivity witnessed for intermolecular cycloadditions.³⁴ This unprecedented reactivity pattern in the intramolecular manifold probably stems from both the noncoplanarity of the C9=C8–C7=O moiety and the marked pyramidalization about the C8 carbon atom in the TSs which leads to greatly diminished conjugative interactions between the tether carbonyl group and the C8=C9 double bond. An energy penalty is thereby incurred in the IMDA reactions involving 9-*E*-substituted stereoisomers, in which conjugation is fully operating in a strain-free environment in the reactants. This energy penalty is less for the 9-*Z*-substituted stereoisomers on account of either diminished conjugation between the tether carbonyl group and the C8=C9 double bond in the reactant (as in the case of **7**), or to diminished steric and electrostatic repulsive interactions in the TS (as in the cases of **16** and **18**).

IMDA precursors carrying an “activating” C1(diene)–OBz substituent were no more reactive than those carrying a “deactivating” C1(diene)–CO₂Me substituent, an alkyl substituent or, indeed, no substituent at all. We recommend caution when making assumptions regarding the “activating” or “deactivating” nature of diene substituents.

The *cis*/*trans*-stereoselectivities and TS asynchronicities of IMDA reactions of substituted pentadienyl acrylates are essentially independent of the nature of C1-diene substituents. This result is seemingly at odds with the results of other workers using 1,3,8-nonatrienes.^{22a} In contrast, the nature and geometry of C9-dienophile substituents have a marked influence upon both the stereoselectivity of these reactions and the degree of asynchronicity in their respective TSs. There is no significant correlation between the degree of TS asynchronicity and *cis*/*trans*-IMDA stereoselectivity.

All IMDA TSs located in this study are asynchronous and furthermore, all exhibit advanced internal bond formation. Advanced internal bond formation is generally thought to give rise to *cis*-selectivity, whereas advanced peripheral bond formation is believed to be the origin of *trans* selectivity.¹ We find that there no correlation between advanced internal/peripheral TS bond development and *cis*/*trans*-selectivity. Instead, IMDA stereoselectivities of pentadienyl acrylates are dominated by subtle yet identifiable TS influences: the strain induced by the folding of the diene-dienophile tether and interactions between the tether and dienophile substituents.

The *cis*-selectivity of the parent pentadienyl acrylate **1** can be explained by considering two opposing effects that operate in the *cis*-TSs: (1) unfavorable eclipsing interactions about the C4–C5 bond, brought about by the C–O–C=O group's strong tendency to achieve local planarity, and (2) attractive interactions between the endo-disposed tether carbonyl group and the diene, perhaps of the Singleton [4+3] SOI kind. The latter is dominant.

Experimental and Computational Methods

IMDA Reactions. Esterification reactions of six different dienols with acryloyl chloride, methyl fumaroyl chloride or monomethyl fumarate, maleic anhydride; diazomethane, *E*-crotonyl chloride, *Z*-crotonic acid, *E*-3-chloroacryloyl chloride, or *Z*-3-chloroacryloyl chloride furnished the requisite triene precursors generally in high yield (see Supporting Information for details). The union of sorbyl alcohol and *Z*-crotonic acid was the exception, with a low isolated ester yield, possibly due to isomerization/polymerization of the acid.³⁸ To avoid [3+2] cycloaddition between diazomethane and the reactive *Z*-alkene dipolarophile, conversion of the dienyl hydrogen maleates to their methyl esters is best performed at low temperature (−78 °C).

Cycloaddition reactions (Table 1) were conducted in dilute toluene or 1,2-dichlorobenzene solutions with a small amount of antioxidant present. Some triene substrates were cyclized in different solvents (e.g., xylenes) and/or under pressure; however, negligible product stereoisomer ratios differences were observed, although there were some differences in isolated yields. The progress of each reaction was monitored by GC and ¹H NMR. Solvents employed, temperatures and reaction times are quoted in Table 1. All cycloadducts were

(38) (a) Rappe, C. In *Organic Syntheses*; Brossi, A., Ed.; John Wiley & Sons Inc.: New York, 1973; Vol. 53, pp 123–127. (b) Wu, W.-J.; Feng, Y.; He, X.; Hofstein, H. A.; Raleigh, D. P.; Tonge, P. *J. Am. Chem. Soc.* **2000**, *122*, 3987–3994.

(39) Wiest, O.; Montiel, D. C.; Houk, K. N. *J. Phys. Chem. A* **1997**, *101*, 8378–8388.

(40) Frisch, M. J.; Trucks, G. W.; Schlegel, H. B.; Scuseria, G. E.; Robb, M. A.; Cheeseman, J. R.; Zakrzewski, V. G.; Montgomery, J. A., Jr.; Stratmann, R. E.; Burant, J. C.; Dapprich, S.; Millam, J. M.; Daniels, A. D.; Kudin, K. N.; Strain, M. C.; Farkas, O.; Tomasi, J.; Barone, V.; Cossi, M.; Cammi, R.; Mennucci, B.; Pomelli, C.; Adamo, C.; Clifford, S.; Ochterski, J.; Petersson, G. A.; Ayala, P. Y.; Cui, Q.; Morokuma, K.; Salvador, P.; Dannenberg, J. J.; Malick, D. K.; Rabuck, A. D.; Raghavachari, K.; Foresman, J. B.; Cioslowski, J.; Ortiz, J. V.; Baboul, A. G.; Stefanov, B. B.; Liu, G.; Liashenko, A.; Piskorz, P.; Komaromi, I.; Gomperts, R.; Martin, R. L.; Fox, D. J.; Keith, T.; Al-Laham, M. A.; Peng, C. Y.; Nanayakkara, A.; Challacombe, M.; Gill, P. M. W.; Johnson, B.; Chen, W.; Wong, M. W.; Andres, J. L.; Gonzalez, C.; Head-Gordon, M.; Replogle, E. S.; Pople, J. A. *GAUSSIAN 98*, Revision A.11; Gaussian, Inc.: Pittsburgh, PA, 2001.

(41) Frisch, M. J.; Trucks, G. W.; Schlegel, H. B.; Scuseria, G. E.; Robb, M. A.; Cheeseman, J. R.; Montgomery, J. A., Jr.; Vreven, T.; Kudin, K. N.; Burant, J. C.; Millam, J. M.; Iyengar, S. S.; Tomasi, J.; Barone, V.; Mennucci, B.; Cossi, M.; Scalmani, G.; Rega, N.; Petersson, G. A.; Nakatsuji, H.; Hada, M.; Ehara, M.; Toyota, K.; Fukuda, R.; Hasegawa, J.; Ishida, M.; Nakajima, T.; Honda, Y.; Kitao, O.; Nakai, H.; Klene, M.; Li, X.; Knox, J. E.; Hratchian, H. P.; Cross, J. B.; Adamo, C.; Jaramillo, J.; Gomperts, R.; Stratmann, R. E.; Yazyev, O.; Austin, A. J.; Cammi, R.; Pomelli, C.; Ochterski, J. W.; Ayala, P. Y.; Morokuma, K.; Voth, G. A.; Salvador, P.; Dannenberg, J. J.; Zakrzewski, V. G.; Dapprich, S.; Daniels, A. D.; Strain, M. C.; Farkas, O.; Malick, D. K.; Rabuck, A. D.; Raghavachari, K.; Foresman, J. B.; Ortiz, J. V.; Cui, Q.; Baboul, A. G.; Clifford, S.; Cioslowski, J.; Stefanov, B. B.; Liu, G.; Liashenko, A.; Piskorz, P.; Komaromi, I.; Martin, R. L.; Fox, D. J.; Keith, T.; Al-Laham, M. A.; Peng, C. Y.; Nanayakkara, A.; Challacombe, M.; Gill, P. M. W.; Johnson, B.; Chen, W.; Wong, M. W.; Gonzalez, C.; Pople, J. A. *Gaussian 2003*, Version B.; Gaussian, Inc.: Pittsburgh, PA, 2003.

recovered unchanged upon re-exposure to the reaction conditions used to form them, demonstrating that the IMDAs reported here are subject to kinetic control.

Cycloadduct Stereochemistry Assignment. Product mixtures of the two (Table 1) diastereomeric cycloadducts were separated by chromatography. The ring junction geometry of each cycloadduct—and hence the (*cis/trans*) mode of cycloaddition from whence it came—was elucidated from the coupling constant between the protons attached to the ring junction carbons. Thus, a $J = 7\text{--}11$ Hz ($H_{ax} - H_{eq}$) coupling constant reveals a *cis*-fused bicycle and a $J = 13\text{--}14$ Hz ($H_{ax} - H_{ax}$) coupling constant indicates a *trans*-fused bicycle. Extensive 2D NMR experiments were carried out to elucidate product stereochemistries and details of these are provided in the Supporting Information. Six crystal structures (Figure 2) confirmed these NMR assignments.

Computations. All TSs were calculated using the B3LYP functional and the 6-31G+(d) basis set, a combination which is known to give acceptable relative energies and geometries.^{2,11,39} All IMDA TSs were located for each molecule studied, including those that are conformational isomers. For example, the benzyloxy and carbomethoxy groups **13** are each capable of adopting either the *s-cis* or *s-trans* conformations,²⁷ thereby producing a total of eight diastereoisomeric TSs (i.e. four *trans*-TSs and four *cis*-TSs). Stereoselectivities for a particular molecule were calculated from the Boltzmann populations at the same temperature that was used experimentally. The Boltzmann population analysis used the (0 K) electronic energies of the TSs, corrected for Zero Point Vibrational Energy (ZPVE; unscaled). A more rigorous treatment, using either enthalpies or free energies of the TSs in place of ZPVE-corrected electronic energies, was not carried out on the grounds that the application of this treatment to cognate IMDAs has previously been found to give similar results to that based simply on electronic energies.¹¹

Full details of the structures (in Cartesian coordinate form) and energies of all computed TSs are given in the Supporting Information. The Gaussian 98⁴⁰ and 03⁴¹ program packages were used throughout.

X-Ray Crystallography. For crystallographic analysis for compounds *trans*-**2P**, *cis*-**6P**, *trans*-**13P**, *trans*-**16P**, *trans*-**17P** and *cis*-**18P** see the Supporting Information.

Acknowledgment. Funding from the Australian Research Council is gratefully acknowledged, as are generous computing time allocations from the Australian Partnership for Advanced Computing and the Australian Centre for Advanced Computing and Communications. We also thank Dr G. A. Jones for some assistance.

Supporting Information Available: Synthetic details, crystallographic data, 2D NMR structure assignments, and the Cartesian coordinates and energies of B3LYP/6-31+G(d) optimized TS geometries. This material is available free of charge via the Internet at <http://pubs.acs.org>.

JO0505829